QuikSCAT Geophysical Model Function and Winds for Tropical Cyclones

Simon H. Yueh*, Bryan Stiles, and W. T. Liu
Jet Propulsion Laboratory, California Institute of Technology, USA

ABSTRACT

A revised geophysical model function for applications of QuikSCAT data to tropical cyclones is described. An analysis of QuikSCAT σ_0s from the fore- and aft-beams indicates a directional dependence of about 0.5-1 dB for above 40 m/s wind speeds. The differences between QuikSCAT fore- and aft-beam σ_0s were used to estimate the second harmonics coefficients, characterizing the upwind and crosswind asymmetry. The results show that the QuikSCAT σ_0s have a peak-to-peak wind direction modulation of ~1 dB at 35 m/s wind speed, and the amplitude of modulation decreases with wind speed. The trend agrees well with the QSCAT1 model function at near 20 m/s. A simple analytic correction of the QSCAT1 model function is presented. We explored two microwave radiative transfer models to account for the attenuation and scattering effects of rain. One is derived from the collocated QuikSCAT and SSM/I data set, and the other one is a published parametric model developed for precipitation radars. The comparison of these two radiative transfer models indicates the relative significance of volume scattering, scattering from rain-roughened surfaces and rain attenuation. The models suggest that the σ_0s of wind-induced surfaces at 40-50 m/s are comparable to the contributions of rain for up to 10-20 mm/h. The radiative transfer models have been used to retrieve the ocean wind vectors from the collocated QuikSCAT and SSM/I rain rate data for several tropical cyclones. The resulting wind speed estimates of these tropical cyclones show improved agreement with the expected wind fields derived from the best track analysis and Holland's model for up to about 15 mm/h rain rate.
Keywords: Scatterometer, hurricane, tropical cyclone, ocean wind, rain scattering, rain attenuation

1. INTRODUCTION

Skillful forecasts of tropical cyclone (TC) track and intensity depend on an accurate depiction of the initial conditions of air and sea states in TC forecast models[1]. A primary source of difficulty in past efforts for TC forecasts has been the inability to make direct observations of the surface wind field, which is one of the key driving forces for the heat and moisture exchanges between the air and sea surfaces[2,3,4].

QuikSCAT, which is officially called the SeaWinds scatterometer on the QuikSCAT satellite, is a spaceborne Ku-band (13.402 GHz) scatterometer and measures the normalized radar cross section (σ_0) of sea surfaces. The ocean surface σ_0 at Ku-band is sensitive to the ocean surface wind velocity (speed and direction). The relationship between σ_0s and the ocean surface wind velocity, usually described by a geophysical model function (GMF), enables the retrieval of ocean surface wind from satellite scatterometer measurements.

QuikSCAT uses a conical scanning antenna reflector, illuminated by two antenna feed horns to produce two antenna beams (Fig. 1). The inner beam operates at a nominal incidence angle of 46° with horizontal polarization and the outer beam operates at a nominal 54°-incidence angle with vertical polarization. During a satellite pass, a wind vector cell (WVC) will be observed at fore- and aft-looking azimuth directions by an antenna beam. The relative azimuth angle between the fore- and aft-looks varies between 0 to 180 degrees, depending on where the WVC is located within the swath. This azimuth diversity was explored to investigate the wind direction dependence of σ_0s for tropical cyclones.

* simon.yueh@jpl.nasa.gov; phone 1 818 354-3012; fax 1 818 393-3077; Jet Propulsion Laboratory, 4800 Oak Grove Drive, Pasadena, CA, USA 91109

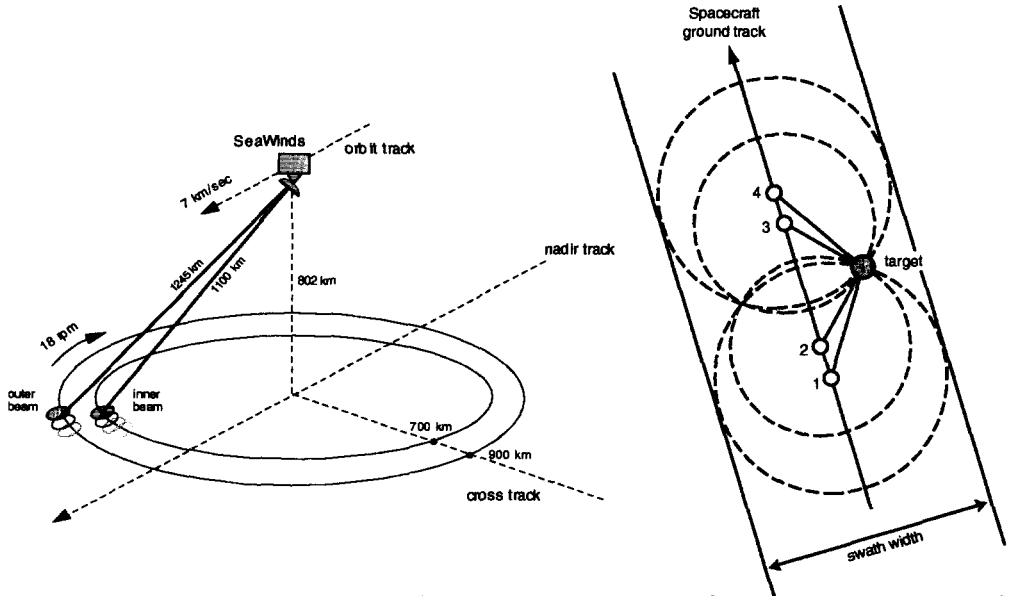

Figure 1. The scanning geometry of the Seawinds scatterometer on the QuikSCAT spacecraft. Two antenna beams enable the sampling a wind vector cell from up to four different azimuth directions.

The QuikSCAT scatterometer has been operating since August 1999 to provide global mapping of ocean winds. It was shown to be accurate for wind speed of up to at least 20 m/s. The global wind fields from QuikSCAT have been routinely assimilated into the numerical weather prediction systems operated by the National Center for Environmental Prediction (NCEP) and European Center for Medium Range Weather Forecast (ECMWF).

The measurement performance of QuikSCAT is uncertain for above 20 m/s wind speeds. The development of the GMF and retrieval algorithm for hurricane wind velocities is still under active research. It has been postulated by Quilfen et al.[5] that three major error sources are limiting the extreme high wind measurement performance of spaceborne scatterometers:

1) deficiencies of the operating GMFs for extreme high winds,
2) effects of rain, including path attenuation, volume scattering from the raindrops, and surface scattering from rain-drop-induced surface roughness, and
3) wind gradient in the sensor footprint near the eyewall where the maximum wind speeds are expected.

Numerous aircraft scatterometer campaigns over tropical cyclones have been performed to assess the scatterometer GMF for extreme high winds. The University of Massachusetts (UMASS) Ku-band scatterometer observations at vertical polarization demonstrated that there were wind speed signals in ocean σ_0s of TCs, although with a reduced sensitivity in comparison with lighter wind conditions (<20 m/s)[6,7]. The dual-polarized observations made by the Jet Propulsion Laboratory (JPL) indicated that the Ku-band radar signature is polarized for hurricane wind conditions with the horizontal polarization being more sensitive to the wind speed than the vertical polarization[8].

An examination of the QuikSCAT σ_0s of several Pacific and Atlantic TCs in 1999 confirmed the reduced wind speed sensitivity and polarized behavior indicated by aircraft observations[9]. In addition, it was suggested that the wind speed sensitivity of σ_0s could extend beyond 40 m/s. However, the limited amount of data did not allow an analysis of wind direction dependence.

This paper presents the results from the analysis of QuiksCAT data from 1999-2000 hurricane seasons with improvements on the wind direction modeling of ocean σ_0s for extreme high winds. To allow a straightforward application of our results, a simple analytic functional correction of the QSCAT1 GMF, presently used by the JPL and

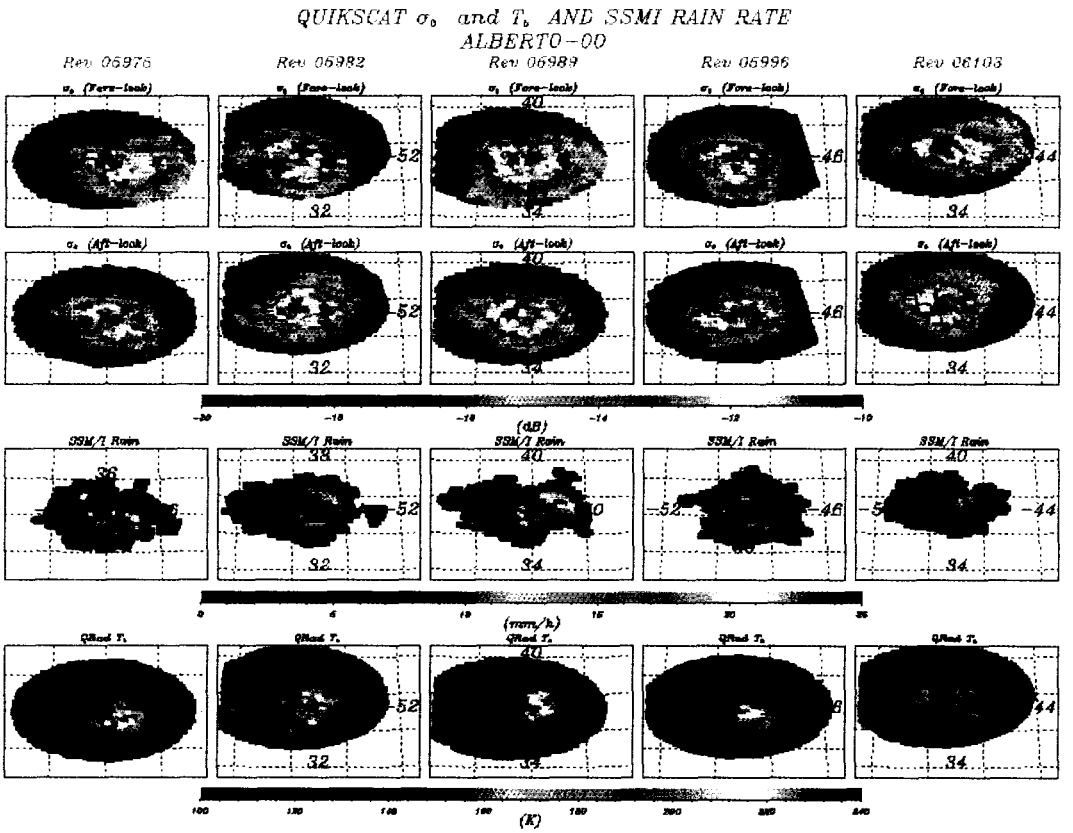

Figure 2. Images of QuikSCAT inner beam σ_0s (rows 1 and 2), SSM/I rain rate (row 3) and QuikSCAT brightness temperature (row 4) for Hurricane Alberto in 2000. Five revs of data are organized in five columns.

National Oceanic and Atmospheric Administration (NOAA) data processing systems, is proposed for rain-free conditions. We also examined two radiative transfer (RT) models to account for the effects of rain. The coefficients of the RT models were taken from previously published research. The RT models present a physical picture regarding the relative significance of rain attenuation, volume scattering and rain-drop-induced surface scattering. The RT models, together with the modified QuikSCAT GMF, were applied to the processing of QuikSCAT data to indicate how accurate the effects of rain can be corrected.

Section 2 discusses the effects of wind direction on QuikSCAT σ_0s of TCs and presents a simple correction model for QSCAT1 GMF. Section 3 describes the radiative transfer models. Section 4 illustrates and discusses the results from the application of the RT model for TC wind retrieval. Summary of our investigation is presented in Section 5.

2. QUIKSCAT σ_0 OBSERVATIONS

The azimuth diversity of QuikSCAT fore- and aft-look geometry allows a direct examination of the wind direction dependence of TC σ_0s. Figure 2 illustrates the fore- and aft-look σ_0s acquired by the inner antenna beam for Hurricane Alberto in 2000. The images, organized in five columns, illustrate the data from five QuikSCAT passes, including revs 5975, 5982, 5989, 5996, 6103. Table 1 summarizes the intensities of Hurricane Alberto derived from the National Hurricane Center best track analyses for these five QuikSCAT passes. The maximum wind speed was near or above 45 m/s.

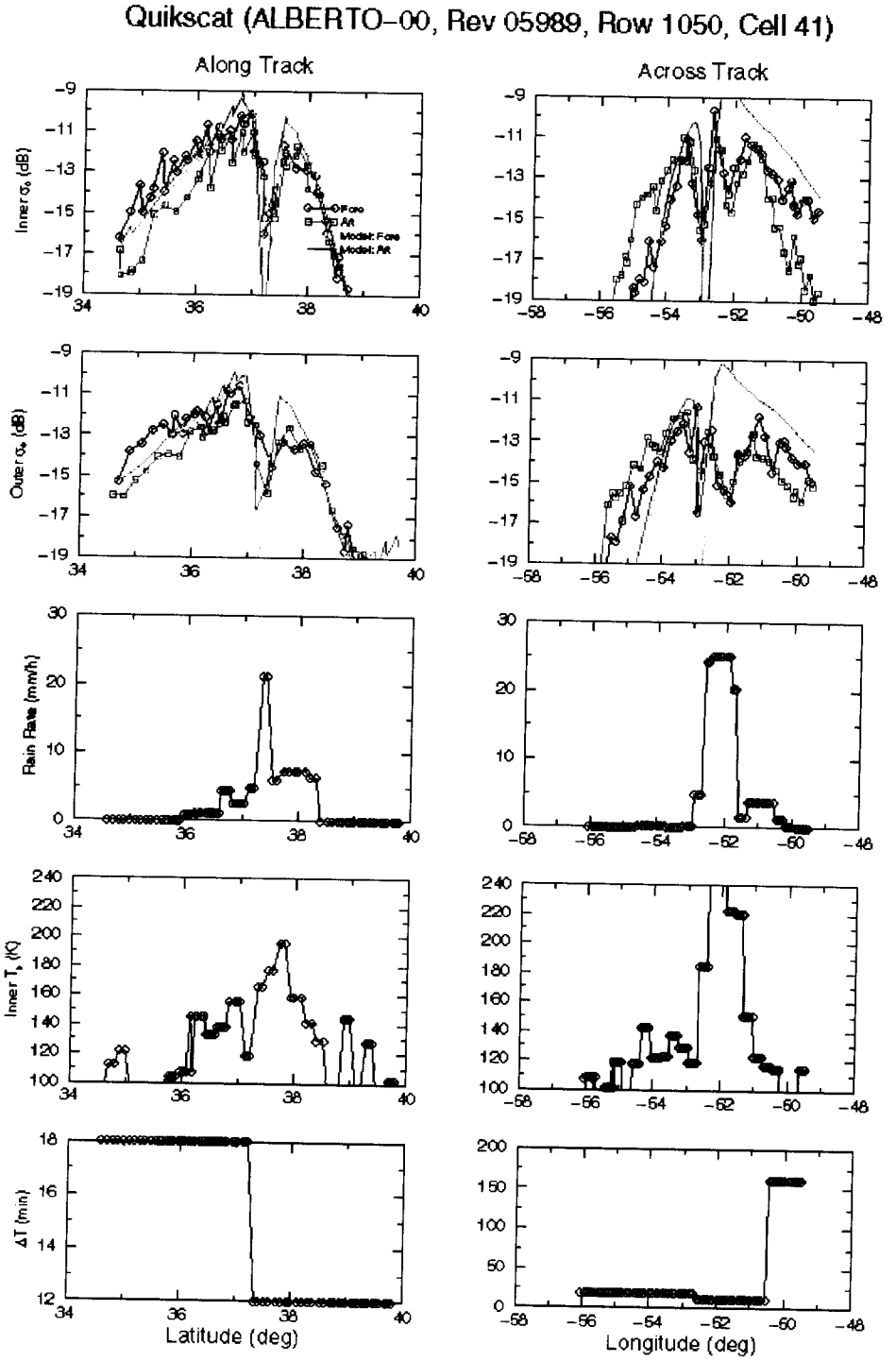

Figure 3. QuikSCAT σ_0s for Hurricane Alberto along and across tracks through the eye of cyclone. The left (right) hand column is for the along (across) track cut of the inner beam σ_0s (first row), outer beam σ_0s (2nd row), SSM/I rain rate (3rd row), QuikSCAT brightness temperature (4th row), and time separation between QuikSCAT and SSM/I observations (5th row).

The σ_0 images of in the first two rows of Fig. 2 indicate the evolution of hurricanes over time with varying spatial pattern. The σ_0 pattern appears asymmetric with respect to the center of cyclone, marked by black crosses. The images in the third row correspond to the collocated rain rate from the Special Sensor Micorwave Imager (SSM/I)[10]. The brightness temperature images (Row 4), derived from the QuikSCAT noise-only measurements, corroborate the spatial distribution of rain rate in the SSM/I images. The regions of high rain rate (>20 mm/h) in columns 2-4 have lower σ_0s than the neighboring areas, apparently resulting from the attenuation effects of rain. Also indicated in the SSM/I images is that many parts of the cyclones could have a rain rate of <10-15 mm/h.

Table 1. Key characteristics of Hurricane Alberto for five QuikSCAT passes. The forward motion velocity and maximum wind speed were derived from the NHC best track analysis. The time difference between the QuiksCAT and the closest SSM/I pass in time is described in column 5.

QuikSCAT Rev	Maximum Wind Speed (m/s)	TC forward motion Speed (m/s), Direction (deg.)	Date/time of QuikSCAT satellite pass (UT)	Time difference between QuikSCAT and SSM/I passes (min)
5975	47	8.6, 33	8/11/2000, 22:15	40
5982	52	8, 55	8/12/2000, 9:31	40
5989	56	9, 66	8/12/2000, 21:49	18
5996	46	8, 75	8/13/2000, 9:06	48
6103	44	1.6, 50	8/20/2000, 9:47	150

It is shown in Fig. 2 that there are differing σ_0s between fore- and aft-look observations. The maximum σ_0s appear to be located to the south of the eyes in the fore-look images for revs 5982, 5989, and 5996. At the same locations, the σ_0s do not appear as strong in the aft-look images. This suggests the influence of wind direction on σ_0s.

Figure 3 illustrates the σ_0s taken from two cuts through the eye of hurricane for rev 5989. The rain rate was mostly less than 10 mm/h on the along track cut with wetter atmosphere on the north side of the eye. To the south of the eye, there is an about 0.5 dB difference between the fore- and aft-look observations. The difference increases with increasing distance from the eye and reaches as large as 3 dB for the inner beam (horizontal polarization) and 2 dB for the outer beam (vertical polarization) at about 200 km off the eye. The results imply that the directional asymmetry of σ_0s decreases with increasing wind speed, but may still have an asymmetry of about 0.5 dB at 40-50 m/s wind speed.

Using the ratios of fore- and aft-look observations, we estimated the upwind and crosswind asymmetry of σ_0s by neglecting the upwind and downwind asymmetry. Specifically, we made the approximation for extreme high wind: $\sigma_0=A_0+A_2\cos(2\phi)$, where ϕ is the relative angle between the wind and antenna look directions. Following the procedure described in a previous publication[9] using the Holland model[15] for hurricane winds to provide the wind speed and direction, we estimated the ratio A_2/A_0 for each pair of fore- and aft-look measurements. The estimates were binned and averaged as function of wind speed and rain rate using data from the QuikSCAT passes of hurricanes in 1999 and 2000.

The estimates of A_2/A_0 ratios are illustrated against the QSCAT1 and NSCAT2 GMF[11] in the two lower panels of Fig. 4. The A_2/A_0 ratios from the QSCAT1 and NSCAT2 GMF are constant at about 1 dB for above 23 m/s wind speed. The constant values were assumptions because of the lack of high wind speed predictions in the numerical weather analyses used to develop the GMFs. Our estimates of A_2/A_0 ratios for 0-2 mm/h and 2-4 mm/h rain bins follow very well with the decreasing trend of QSCAT1 and NSCAT A_2/A_0 ratios at near 20 m/s wind speeds.

From the QuikSCAT estimates, we propose the following modifications to the QSCAT1 GMF for wind speeds above 23 m/s:

$A_i/A_0 = A_i/A_0$ (QSCAT1 at 23 m/s) * $\{1-\exp[-(25/w)^2]\}/\{1-\exp[-(25/23)^2]\}$ for $i \geq 1$, and

$A_0 = A_0$ (QSCAT1 at 23 m/s) + $\beta(w-23)$

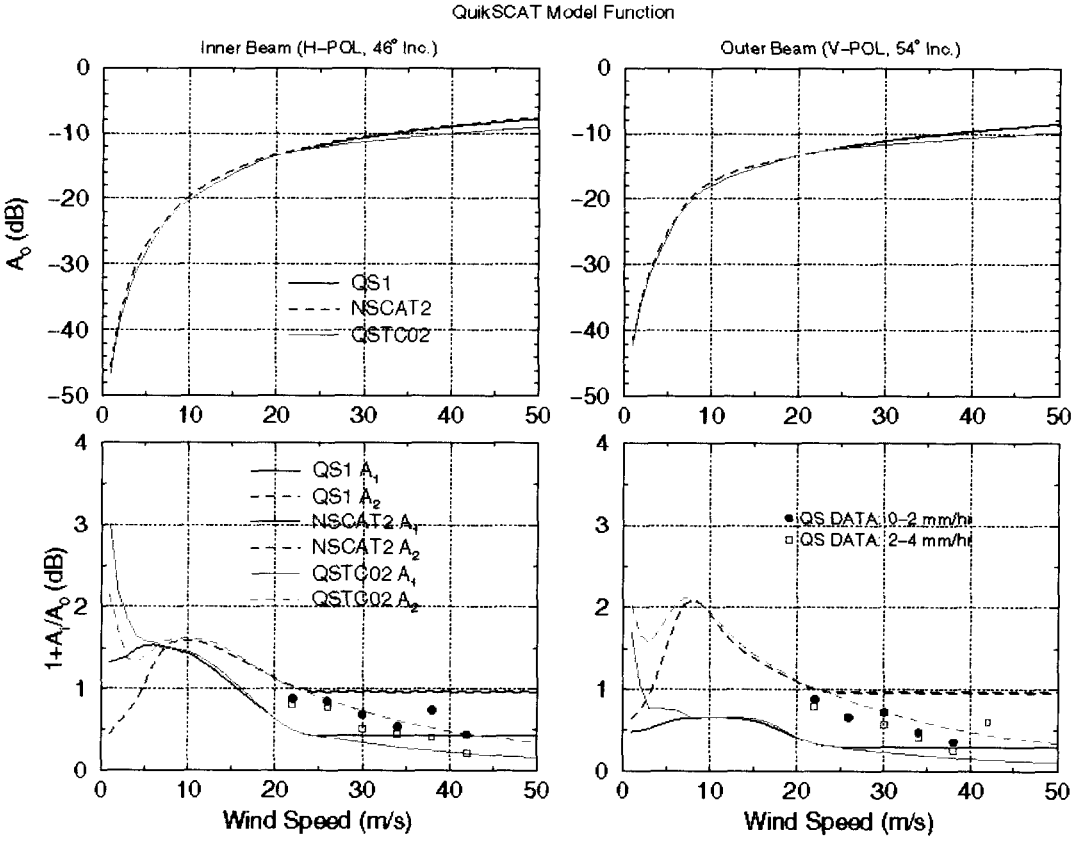

Figure 4. QuikSCAT A_0, A_1 and A_2 coefficients versus wind speed. QSCAT1 GMF coefficients are labeled by QS1, NSCAT2 GMF by NSCAT2, revised QSCAT GMF by QSTC02.

Here 'w' is the wind speed in m/s. The amplitude of β is taken from previous analysis[9] with β=0.0025 for inner beam and 0.0018 for outer beam. The modified GMF is illustrated in Fig. 4 with curve label, 'QSTC02'.

3. RADIATIVE TRANSFER MODELING

Rain will attenuate the radar signal, introduce volume scattering from raindrops, and roughen the water surface to enhance the surface scattering at Ku-band frequencies. To account for the effects of rain, we assume the following radiative transfer model for QuikSCAT observations:

$$\sigma_0 = \sigma_{0RV} + \exp(-2kH/\cos\theta)(\sigma_{0WIND} + \sigma_{0RS})$$

Here σ_{0RV} represents the volume scattering from raindrops, 'k' the attenuation per unit length, and σ_{0RS} surface scattering from rain-induced surface roughness. σ_{0WIND} is the QSCAT GMF for rain-free conditions.

The above model assumes a stratified rain layer with constant rain rate 'R' and column height of H. For this model, the two-way rain attenuation factor at an incidence angle of θ is accounted for by the exponential factor. The volume scattering is related to the rain reflectivity (Z) by:

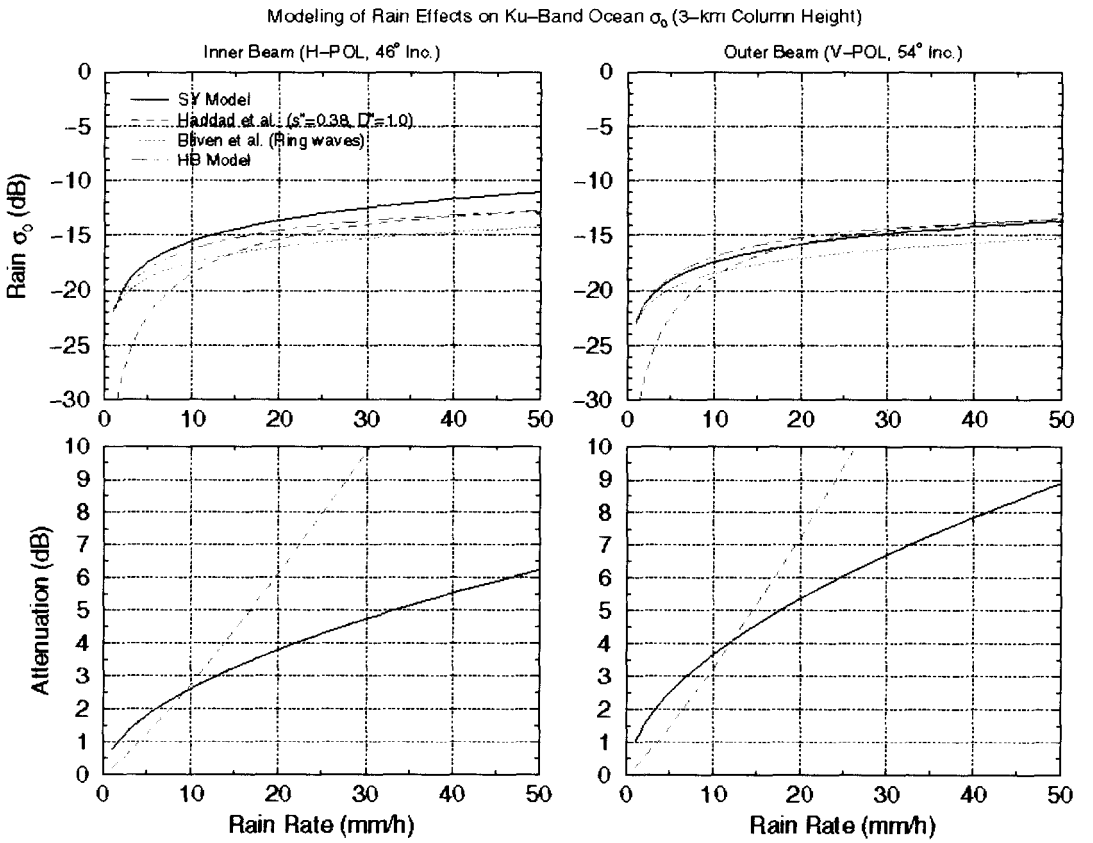

Figure 5. Illustrations of radiative transfer models for rain published by Stiles and Yueh (SY), Haddad et al. for volume scattering and rain attenuation, Bliven et al. for ring waves induced by raindrops, and comined Haddad and Bliven's model (HB).

$\sigma_{0RV} = Z*H*0.9\pi^5/\lambda^4*[1-\exp(-2kH/\cos\theta)]/(2kH/\cos\theta)$

Here λ is the radar wavelength.

3.1 HB Model

The dependence of Z and k on the rain rate R typically takes a power-law form. The parametrization developed by Haddad et al.[12] are used to model Z and k. With the shape parameters "D=1.0" and "s=0.38", $Z=185.01*R^{1.504}$ and $k=0.223*R^{1.156}$.

The scattering by the water surfaces roughened by raindrops has also found to be related to the rain rate by a power law form. Following the model proposed by Bliven et al.[13], $\sigma_{0RS}=0.0063R^{0.46}$ for the QuikSCAT inner beam and $0.0050R^{0.46}$ for the QuikSCAT outer beam. Here the power law exponent of 0.46 was from Bliven et al.[13], but the proportional coefficients, 0.0063 and 0.0050, were determined by matching the modeling outputs at 1 mm/h with the rain scattering model suggested by Stiles and Yueh[14] (see upper panels of Fig. 5).

We will denote the above radiative transfer model with key modeling elements from Haddad et al.[12] and Bliven et al.[13] as the HB model.

3.2 SY Model

In addition to the HB model, we applied another rain scattering model for the correction of rain effects on wind retrieval. This model was proposed by Stiles and Yueh[14] and will be denoted as the SY model. The SY model was developed based on the analysis of collocated QuikSCAT data, NCEP wind and SSM/I rain rate. In principle, the SY model is applicable to <20 m/s wind speed and <25mm/h rain rate conditions because of the limitations of NCEP winds (very few high wind predictions) and SSM/I rain rate (saturated at 25 mm/h). The use of SY model for tropical cyclones is an extrapolation. The SY model does not distinguish the volume scattering and surface scattering induced by raindrops and takes the following form:

$\sigma_0 = A + B\sigma_{0WIND}$

The coefficients, A and B, are parameterized by the integrated rain rate 'RH': $A = 0.0032\ (RH)^{0.64}$ for the inner beam and $0.0029\ (RH)^{0.54}$ for the outer beam. $B = \exp[-0.096\ (RH)^{0.54}]$ for the inner beam and $\exp[-0.13\ (RH)^{0.55}]$ for the outer beam. Note that the unit of H here is km, instead of m used for the HB model.

Figure 5 compares the model predictions of A and B from the HB and SY models for a rain layer with a thickness of 3 km. The upper two panels illustrate the coefficient 'A' (rain σ_0) for the inner and outer beams. The agreement between SY (solid curve) and HB (short-long dashes) is reasonable for <10 mm/h, but could be different by as much as 2 dB at 50 mm/h rain rate for the inner beam. In the HB model, σ_{0RS} for the scattering by rain-induced surface roughness is more significant than the volume scattering for <10 mm/h rain rate, but become less significant for > 15 mm/h.

The major discrepancy between the SY and HB models is the estimates of two-way attenuation, illustrated in the two lower panels of Fig. 5. The HB model predicts lower attenuation for <10-mm/h rain rate, but grows more rapidly for higher rain rates. This could be a result of difference in spatial resolution. The HB model for attenuation was derived from the aircraft rain radar data with resolution in the order of km, while the SY model was an empirical analysis of QuikSCAT and SSM/I data with a footprint size in the range of 30-40 km. A large footprint size could result in partial beam filling of rain cells, leading to a more gentle increase of attenuation versus rain rate[10]. Here we will not attempt to resolve the differences between these two models, but will use them to indicate the sensitivity of wind retrievals to rain models.

4. QUIKSCAT WIND RETRIEVAL FOR TROPICAL CYCLONES

The SY and HB radiative transfer models, together with the revised rain-free GMF, have been applied to the wind retrievals for hurricanes in 1999 and 2000. The methodology for wind retrieval is based on the maximum likelihood measure to minimize the difference between QuikSCAT σ_0 measurements and model estimates under the constraint of SSM/I rain rates. In general, there are multiple local minima, representing multiple possible solutions (ambiguities). We used the Holland model field to select the closest wind direction ambiguity[9].

Figure 6 illustrates the wind fields for Hurricane Alberto retrieved from QuikSCAT rev 5982 data. The upper left panel plots the wind field for the selected wind ambiguity from the JPL QuikSCAT ground data processing system. The maximum wind speed was about 35 m/s, far smaller than the 52 m/s maximum wind speed indicated by the best track analysis (Table 1). The upper right panel plots the wind speed of the closest wind ambiguities with respect to the Holland model field, which was generated using the NHC best track analysis and the radius to maximum wind indicated in the QuikSCAT σ_0 data. The closest ambiguity offers small increase of wind speeds for several WVCs to the south of eyewall, but the maximum wind speed is still underestimated. The middle left panel illustrates the NCEP forecasts, which has a poor representation of the hurricane.

The middle right panel of Fig. 6 plots the wind field retrieved using the SY model and revised GMF, and has indicated stronger wind speeds to the south of eyewall than the upper right panel. However, the wind speeds for the region to the

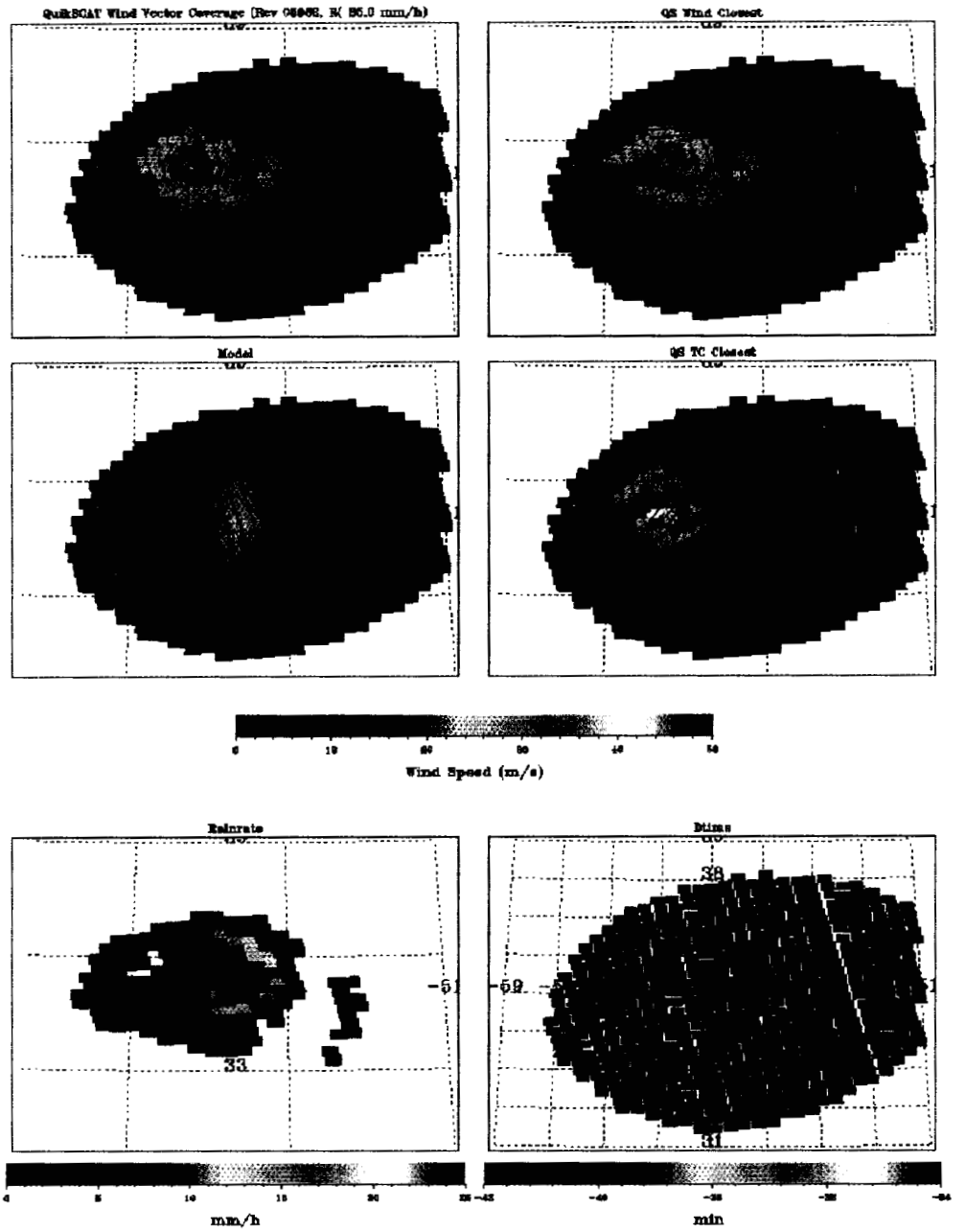

Figure 6. QuikSCAT winds for Hurricane Alberto from rev 5982. The upper left panel plots the wind field of the selected direction ambiguity from the JPL ground data processing system using the QSCAT1 GMF and upper right panel the closest ambiguity field. The NCEP wind is in the middle left panel. The wind field from the retrievals using SY-model is in the middle right panel. The bottom panels are the SSM/I rain rate and time difference from the QuikSCAT observations.

east of eyewall, indicated by high SSM/I rain rate (orange color in the lower left panel), appear to be underestimated.

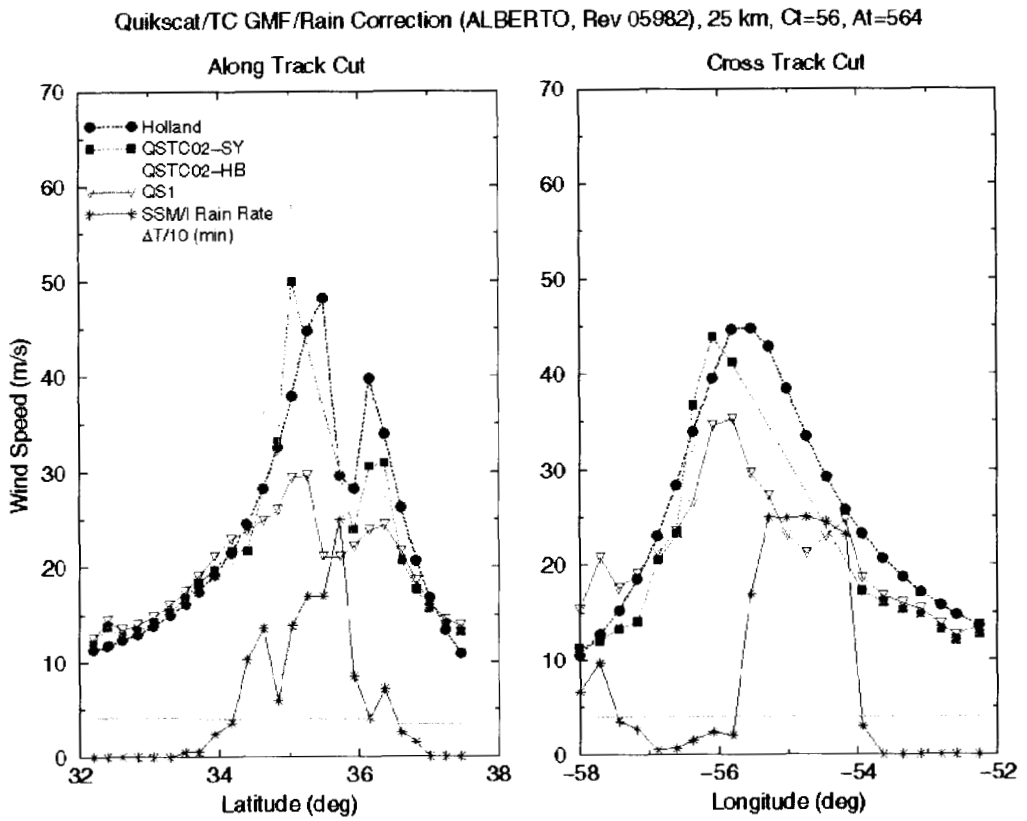

Figure 7. The wind speed profiles of Hurricane Alberto (QuikSCAT rev 5982) along and across track through the center of cyclone. The JPL ground data processing system output fields are labeled by QS1, wind retrievals using the SY-model by QSTC02-SY, wind retrievals using the HB-model by QSTC02-HB. The SSM/I rain rate is in mm/h. The difference between SSM/I and QuikSCAT observation times is divided by 10 for illustration.

Similar characteristics have been observed in the wind retrievals for other revs of QuikSCAT hurricane passes. The results indicate that the SY model performs reasonably well for relatively light rain (<10 mm/h), but performs poorly for above 15 mm/h.

Figure 7 plots the wind speeds along two cuts through the eye of Alberto: One is along track and the other is across track. The wind speed retrievals from the SY model seem to have the best agreement with the Holland model field. The wind retrievals from the HB model overshoot the wind speed on the eyewall. Note that the wind speeds from the SY or HB models for the regions with >15 mm/h rain rate were not included in the plots, because they were significant underestimates or overestimates.

5. SUMMARY

This paper describes a revised QuikSCAT GMF for applications to tropical cyclones. The primary corrections are the wind direction dependence of the σ_0 for >23 m/s wind speed. A direct examination of the QuikSCAT σ_0 data from several intense storms indicates a directional asymmetry of about 0.5-1 dB for wind speeds in the range of 40-50 m/s. The fore- and aft-look differences of σ_{0s} are used to estimate the amplitude of A_2 versus wind speed. The QSCAT1 A_2 coefficients, characterizing the upwind and crosswind asymmetry, level off at above 23 m/s, while the A_2 coefficients

derived from the data decrease with increasing wind speed and appear to match well with the decreasing trend of the QSCAT1 A_2 coefficients at near 20 m/s. The corrections to the QSCAT1 GMF are expressed in a simple analytic form for ease of use.

To compensate for the effects of rain on wind retrieval, two radiative transfer models are examined. The predictions of scattering from raindrops and rain-roughened surfaces agree reasonably well between these two models, but there is a significant difference in the predictions of rain attenuation. Both models are applied to the processing of the QuikSCAT winds and improve the estimates of wind speed for relatively light rian. However, the results are unsatisfactory for high rain rate (>15 mm/h). Nevertheless, the collocated analysis of SSM/I rain rate indicates that many TCs have <15 mm/h rain rate over a larger portion of the cyclone, and the described RT models will make positive impact to the wind speed estimates of these regions.

ACKNOWLEDGMENTS

The research carried out in this paper is performed by the Jet Propulsion Laboratory under a contract with the National Aeronautics and Space Administration. The research is supported by the NASA research fund for the Ocean Vector Wind Science Team. We are grateful to M. Freilich and B. Vanhoff of the Oregon State University and F. Wentz of Remote Sensing Systems for making the collocated SSM/I products available for this investigation.

REFERENCES

1. Bender, M. A., R. J. Ross, R. E. Tuleya, and Y. Kurihara, Improvements in Tropical cyclone Track and Intensity Forecasts Using the GFDL Initialization System, *Monthly Weather Review,* Vol. 121, pp. 2046--2061, 1993.
2. Dickinson, S. and R. A. Brown, "A Study of Near-Surface Winds in Marine Cyclones Using Multiple Satellite Sensors," *J. Appl. Meteorology,* Vol.~35, 769-781, June 1996.
3. Hsu, C. S., W. T. Liu, and M. G. Wurtele, "Impact of Scatterometer Winds on Hydrologic Forcing and Convective Heating Through Surface Divergence," *Monthly Weather Review,* Vol.~125(7), 1556-1576, July 1997.
4. Liu, W. T., Hua Hu, and Simon Yueh, "Quikscat and TRMM Reveal the Interplay Between Dynamic and Hydrologic Parameters in Hurricane Floyd," *EOS Trans.,* American Geophysical Union, Vol. 81, No. 23, 253, 257, June 6, 2000.
5. Quilfen, Y., B. Chapron, T. Elfouhaily, K. Katsaros and J. Tournadre, "Observation of Tropical Cyclones by High-Resolution Scatterometry," *J. Geophys. Res.,* 103(C4), 7767-7786, April 1998.
6. Carswell, J., S. C. Carson, R. E. McIntosh, F. K. Li, G. Neumann, D. J. Mclaughlin, J. C. Wilkerson, P. G. Black, and S. V. Nghiem, "Airborne Scatterometers: Investigating Ocean Backscatter Under Low- and High-Wind Conditions," *Proc. IEEE.* Vol. 82, No. 12, 1835--1860, 1994.
7. Donneley, W. J. J. R. Carswell, R. E. McIntosh, P. S. Chang, J. Wilkerson, F. Marks, and P. G. Black, "Revised ocean backscatter models at C and Ku-band under high wind conditions," *J. Geophys. Res.,* 104, pp. 11,485-11,497, 1999.
8. Yueh, S. H., R. West, F. Li, W.-Y. Tsai and R. Lay, "Dual-Polarized Ku-band Backscatter Signatures of Hurricane Ocean Winds," *IEEE Geosci. and Remote Sens.*, Vol. 38, No. 1, 73-88, January 2000.
9. S. H. Yueh, B. W. Stiles, W.-Y. Tsai, H. Hu, W. T. Liu, "QuikSCAT Geophysical Model Function for Tropical Cyclones and Applications to Hurricane Floyd," *IEEE Trans. Geosci. Remote Sens.,* Vol. 39, No. 12, pp. 2601-2612, 2001.
10. Wentz, F. J., and R. W. Spencer, "SSM/I Rain Retrievals within a Unified All-Weather Ocean Algorithm," *J. Atmospheric Sci.,* Vol.~55, No.~6, 1613--1627, 1998.
11. Wentz, F. J., M. H. Freilich, and D. K. Smith, "NSCAT-2 Geophysical Model Function," *Proc.~of 1998 Fall AGU Meeting*, San Francisco, 1998.
12. Z. S. Haddad, D. A. Short, S. L. Durden, E. Im, S. Hensley, M. Grable, R. A. Black, "A New Parametrization of the Rain Drop size Distribution," *IEEE Trans. Geosci. Remote Sens.,* Vol. 35, No. 3, pp. 532-539, 1997.
13. L. F. Bliven, P. W. Sobieski, and C. Craeye, "Rain generated ring-waves: measurements and modeling for remote sensing," *Int. J. Remote Sens.,* Vol. 18, No. 1, pp. 221-228, 1997.

14. B. Stiles and S. Yueh, "Impact of Rain on Wind Scatterometer Data," *IEEE Trans. Geosci. Remote Sens.*, in press, 2002.
15. Holland, G., "An Analytic Model of the Wind and Pressure Profiles in Hurricanes," *Monthly Weather Review,* Vol. 108, pp. 1212-1218, 1980.